miR-486 Expression is Regulated by DNA Methylation in Osteosarcoma

Heidi Namløs
Oslo University Hospital
Magne Skårn
Oslo University Hospital
Deeqa Ahmed
Oslo University Hospital
Iwona Grad
Oslo University Hospital
Kim Andresen
Oslo University Hospital
Stine Kresse
Oslo University Hospital
Massimo Serra
Istituto Ortopedico Rizzoli
Katia Scotlandi
Istituto Ortopedico Rizzoli
Antonio Llombart-Bosch
University of Valencia
Ola Myklebost
Oslo University Hospital
Guro Lind
Oslo University Hospital
Leonardo Meza-Zepeda (Leonardo.Meza-Zepeda@rr-research.no)
Oslo University Hospital

Research Article

Keywords: tumour, patient, DNA, cell

Posted Date: December 3rd, 2020

DOI: https://doi.org/10.21203/rs.3.rs-112581/v1

miR-486 expression is regulated by DNA methylation in osteosarcoma

Short title: Epigenetic regulation of miR-486 in osteosarcoma

Heidi M. Namløs[1], Magne Skårn[1], Deeqa Ahmed[2], Iwona Grad[1], Kim Andresen[2], Stine H. Kresse[1], Massimo Serra[3], Katia Scotlandi[3], Antonio Llombart-Bosch[4], Ola Myklebost[1,5], Guro E. Lind[2], Leonardo A. Meza-Zepeda[1,6*]

[1]Department of Tumor Biology, Institute for Cancer Research, The Norwegian Radium Hospital, Oslo University Hospital, Oslo, Norway. [2]Department of Molecular Oncology, Institute for Cancer Research, The Norwegian Radium Hospital, Oslo University Hospital, Oslo, Norway. [3]IRCCS Istituto Ortopedico Rizzoli, Laboratory of Experimental Oncology, Bologna, Italy. [4]Department of Pathology, Valencia University, Valencia, Spain. [5]Department for Clinical Science, University of Bergen, Norway. [6]Genomics Core Facility, Department of Core Facilities, Institute for Cancer Research, Oslo University Hospital, Oslo, Norway.

[*]Corresponding author: Leonardo A. Meza-Zepeda, Inst. for Cancer Research, Oslo University Hospital, PO box 4953 Nydalen, 0424 Oslo, Norway. Leonardo.Meza-Zepeda@rr-research.no. Phone/Fax: +47-99035706 /+47-2278 1795

Abstract

Osteosarcoma is the most common primary malignant tumour of bone occurring in children and young adolescents, and is characterised by complex genetic and epigenetic changes. The miRNA miR-486-5p has been shown to be downregulated in osteosarcoma and in cancer in general. To investigate if the *miR-486* locus is epigenetically regulated, we integrated DNA methylation and miR-486-5p expression data using cohorts of osteosarcoma cell lines and patient samples. An upstream CpG island of *mir-486* was shown to be highly methylated in osteosarcoma cell lines as determined by methylation-specific PCR and direct bisulfite sequencing. High methylation levels were seen for osteosarcoma patient samples, cell xenografts and cell lines based on quantitative methylation-specific PCR. 5-Aza-2'-deoxycytidine treatment of osteosarcoma cell lines caused induction of miR-486-5p in osteosarcoma cell lines. When overexpressed, miR-486-5p affected cell morphology. miR-486-5p represents a highly cancer relevant, epigenetically regulated miRNA in osteosarcoma.

Introduction

High-grade osteosarcoma is the most prevalent primary malignant tumour of bone, affecting both children, adolescents and, more rarely, elderly people. Following the introduction of multi-agent chemotherapy in the 1970s, the 5-year survival rate increased considerable reaching 60-70% among patients with conventional high-grade osteosarcoma [1] However, advances in treatment have stalled with no further improvement in survival [2], and also exhibit a collateral risk for adverse toxicity events. Improved biological knowledge is required to develop new treatment opportunities and further improve the survival of osteosarcoma patients.

Osteosarcoma is characterized by considerable phenotypic and genomic heterogeneity, and few recurrent targetable genetic changes have been reported. Osteosarcoma exhibits a complex karyotype with high genetic and chromosomal instability seen as multiple rearrangements across the genome, kataegis and chromothripsis [3-6]. The genetic markers identified have been associated with treatment response and prognosis, thus appearing as promising candidates for a translation to clinical practice [7,8]. However, the limited extent of recurrent profiles identified indicates that a substantial regulation of the transcriptional programs in osteosarcoma may rather be caused by epigenetic programs [9-13], providing novel avenues for cancer therapy[14].

Epigenetic mechanisms are fundamental drivers of tumour initiation, development and progression [15]. Several epigenetic alterations have been identified, including biomarkers for various diseases [16]. DNA methylation is the most commonly studied epigenetic alteration in cancer [17], comprising covalent addition of methyl groups to CpG sites. CpG islands are characterized by regional enrichment of CpG sites and are present in approximately 70% of all human gene promoters [18]. In normal cells, these CpG islands are usually unmethylated. In cancer, however, CpG island hypermethylation is frequently observed, accompanied by long-term silencing of gene expression [19].

MicroRNAs (miRNAs) are a key class of epigenetic regulators as they act to post-transcriptionally silence large numbers of genes without modifying the DNA [20]. miRNAs are frequently associated with CpG islands and are themselves also found silenced through epigenetic mechanisms [21]. Dysregulated miRNA expression may result in aberrant expression of genes that play critical roles in osteosarcoma tumorigenesis and progression [22-25]. We have previously identified miR-486-5p to be among the most downregulated miRNAs in osteosarcoma cell lines [24], and miR-486 has also been shown to be downregulated in osteosarcoma patient samples compared to normal samples [26]. However, the mechanism of repression of miR-486-5p is still unknown in osteosarcoma. Given that epigenetic regulation of miR-486-5p has been described in lung cancer [27], we hypothesized that this could be the mechanism of miR-486-5p regulation also in osteosarcoma.

In an effort to advance the understanding of osteosarcoma biology, we investigated if the expression of miR-486-5p was epigenetically regulated through methylation of promoter regions. We analysed miR-486-5p expression and DNA methylation levels in a cohort of osteosarcoma cancer cell lines and patient samples. Qualitative and quantitative methylation analyses were performed, allowing us to characterize the *mir-486* locus in detail. Finally, the *in vitro* effect of *miR-486* overexpression on cell morphology and proliferation was investigated.

Materials and Methods

Osteosarcoma cell lines, xenografts, patient samples and normal controls. A panel of human osteosarcoma cell lines (n=21) composed of 143B, CAL-72, G-292, HAL, HOS, IOR/MOS, IOR/OS9, IOR/OS10, IOR/OS14, IOR/OS15, IOR/OS18, IOR/SARG, KPD, MG-63, MHM, MNNG/HOS, OHS, OSA, Saos-2, U-2 OS and ZK-58 were obtained from ATCC (www.lgcstandards-atcc.org), DSMZ (http://www.dsmz.de/) or research partners in the EU funded EuroBoNeT project [28]. These cell lines have been extensive characterised at the molecular and phenotypic level [10,29] and authenticated through STR testing.

The xenograft cohort comprised osteosarcoma xenografts established at the Norwegian Radium Hospital (n=19) and at the University of Valencia (n=22) [30,31]. In short, human tumours were implanted subcutaneously in nude mice and passed successively.

The osteosarcoma patient sample panel comprised fresh-frozen tissue from 30 high-grade osteosarcoma samples collected at the Norwegian Radium Hospital (n=21) and at the University of Valencia (n=9). The tumours were diagnosed by an osteosarcoma pathologist, according to the current World Health Organization classification [32].

Six bone samples were used as normal controls. Normal bones were purchased from Capital Biosciences (Capital Biosciences, MD, USA) (n=2) or obtained from amputations of cancer patients at the Norwegian Radium Hospital (n=4), where bone samples were collected distant from the tumour margin. DNA copy number analysis of the latter four samples (Bone 1-4) showed normal diploid karyotype [10].

Ethics declaration and approval for animal experiments

The project was approved by the Ethical Committee of Southern Norway (Project S-06132) and the Institutional Ethical Committee of Valencia University, and informed consent is available for the patients. Animal experiments were performed according to protocols approved by the

National Animal Research Authority in compliance with the European Convention of the Protection of Vertebrates Used for Scientific Purposes (approval ID 1499 and 3275). All methods were performed in accordance with the relevant guidelines and regulations.

miRNA expression profiling. Total RNA from osteosarcoma cell lines and bones was extracted and quality controlled as previously described [24]. miRNA expression profiling was performed using the Agilent miRNA Complete Labeling and Hyb Kit Version 2.0, and Agilent Human miRNA Microarrays (version 2, 799 human miRNAs). miRNA data was imported into GeneSpring GX10 (Agilent Technologies Inc., CA, USA), and the intensity values were $\log_2$ transformed and quantile normalized. MIAME (minimum information about a microarray experiment) compliant data can be downloaded from the GEO repository (www.ncbi.nlm.nih.gov/geo/), accession number GSE28425.

DNA methylation profiling. DNA was isolated using the Wizard Genomic DNA Purification Kit (Promega, WI, USA). For the initial analyses, DNA methylation profiling of 19 cell lines and four bone samples was performed using the Illumina HumanMethylation27 BeadChip (Illumina Inc., California, USA), covering 27,000 CpG sites across the genome [10]. For an extended validation, DNA methylation profiling was performed on 10 additional patient samples and four bone samples using the Infinium HumanMethylation450 BeadChip from Illumina, covering 485,000 CpG sites across the genome. Data extraction and initial quality control of the bead summary raw data were performed using GenomeStudio V2011.1 and the Methylation module v1.9.0, both provided by Illumina. For each sample, Beta values for each probe (average ratio of signal from methylated probe relative to the sum of both methylated and unmethylated probes) were exported for downstream analysis.

Integration of miRNA and methylation data. The association between CpG methylation and miRNA expression data in osteosarcomas and normal samples was calculated using Pearson's Correlation between miR-486-5p expression and methylation level (Beta) using the Methylation module v1.9.0 of GenomeStudio. DeltaBeta values for the groups of samples were calculated (Beta for cell lines minus Beta for normal samples).

Quantitative real-time reverse-transcription PCR (qRT-PCR). qRT-PCR was performed using the ABI PRISM 7500 DNA Sequence Detection System (Life Technologies, CA, USA). TaqMan MicroRNA Reverse Transcription Kit and TaqMan MiRNA Assays (Life Technologies) were used to generate cDNA and to quantitatively detect the expression of mature miR-486-5p. For activin A receptor like type 1 (*ALK1*) expression quantification, the Fast Cells-to-Ct reagents (Life Technologies) were used to generate cDNA. Transcript-specific TaqMan Gene Expression Assays (Life Technologies) were used for quantitative PCR. Gene expression was normalized towards *RNU44* for miRNA quantification and glyceraldehyde 3-phosphate dehydrogenase (*GAPDH*) for *ALK1* quantification. Overview of TaqMan assays are found in Supplementary Table 1. The relative expression levels were determined using the comparative C_T method.

5-Aza-2'-deoxycytidine treatment. Osteosarcoma cells were cultured in the presence of 1 µM of 5-Aza-2'-deoxycytidine (5-Aza) (Sigma-Aldrich MO, USA), as previously described [10]. The cells were harvested after 72 hours and total RNA was isolated using the miRNeasy Mini Kit (Qiagen, Germany).

DNA extraction and bisulfite conversion. Genomic DNA from tumour and normal samples was isolated by standard phenol chloroform extraction or using the Wizard Genomic DNA

Purification Kit (Promega). DNA (1.3 μg) was bisulfite treated using the EpiTect Bisulfite Kit (Qiagen), and purified using the QIAcube (Qiagen).

Qualitative methylation-specific polymerase chain reaction (MSP). Primers for MSP were designed using Methyl Primer Express 1.0 (Life Technologies) (Supplementary Table 2). The MSP was carried out using approximately 24 ng of bisulfite treated DNA, and performed as previously described [33]. All results were verified with a second round of MSP and scored independently by two of the authors.

Direct DNA bisulfite sequencing. A subset of the osteosarcoma cell lines was subjected to direct bisulfite sequencing as previously described [34], allowing for a semi-quantitative visualization of 5-methylcytosines. The *mir-486* primers were designed using the Methyl Primer Express 1.0 (Life Technologies) and flanked the MSP amplicons (Supplementary Table 2). The approximate degree of methylation at each CpG site was calculated by comparing the peak height of the cytosine signal to the sum of cytosine and thymine peak height signals as previously described [35]. CpG sites with ratios between 0-0.2 were classified as unmethylated, CpG sites with ratios in the range of 0.21-0.8 were classified as partially methylated, and CpG sites with ratios from 0.81-1.0 were classified as hypermethylated.

Quantitative methylation-specific polymerase chain reaction (qMSP). A quantitative qMSP analysis was carried out using approximately 30 ng of bisulfite-treated DNA and performed as previously described [33]. Commercially available fully methylated DNA (CpGenome Universal Methylated DNA, MA, USA), unconverted and bisulfite-treated normal DNA were included as controls. Primers and probes were designed using Primer Express Software 3.0 (Life Technologies) (Supplementary Table 2). The *ALU-C4* repetitive element was used as an

internal reference, and the values were calculated as percent of methylated reference (PMR) [36]. The median gene:Alu ratio of each gene was divided by the median gene:Alu ratio of the positive control and multiplied by 100. To ensure high specificity for each qMSP assay, the thresholds for scoring the osteosarcoma samples as methylated were set according to the highest PMR value across the test series of normal bone. Samples with PMR values equal to or above the scoring threshold were considered to be methylated.

Transfection with synthetic miRNAs and live cell imaging. Cells were seeded at a density of 1,250-2,500 cells per well in 96-well plates the day before transfection. Synthetic miR-486-5p mimics and Negative Control #1 (PM10546 and AM17110, respectively, Life Technologies) were transiently transfected into osteosarcoma cells at a final concentration of 15 nM using the INTERFERin siRNA transfection reagent (Polyplus-transfection SA, France). The cellular growth after transfection was measured every three hours, by a live-cell imaging system, IncuCyte ZOOM (Essen Bioscience, UK) and the percent of cells confluence was calculated with the corresponding software application (version 2013BRev1).

Statistics. Analyses were performed with the GraphPad Prism 5 software. Non-parametric Mann-Whitney U test was applied to compare groups of samples. P-values were derived from two-sided tests using a significance level of 0.05. Similarities between samples were calculated using Pearson's correlation (r). Statistical differences between the group of cell lines before and after 5-Aza treatment were calculated using a paired t-test.

Results

Low expression of miR-486-5p in osteosarcoma

To follow up on our earlier observations of miR-486 expression in osteosarcoma [24], miR-486-5p expression level was examined in a panel of osteosarcoma patient samples (n=10), osteosarcoma cell lines (n=17) and normal bone samples (n=4) by qRT-PCR. The mean expression of miR-486-5p was reduced 5-fold in patient samples ($p<0.01$) and 340-fold in cell lines ($p<0.001$) compared to normal bone (Figure 1a). This confirms a low expression of miR-486-5p in osteosarcoma using both patient tissue samples and cell lines.

DNA methylation is associated with low expression of *miR-486* in osteosarcoma cell lines

miR-486-5p is encoded within the last intron of the *ANK1* gene. The methylation level of *ANK1* was quantified in osteosarcoma cell lines (n=19) and normal bone samples (n=4) using Illumina HumanMethylation27 BeadChips. This microarray contain one CpG site in the CGI CpG79 (chr8:41654876-41655984), covering the transcriptional start site (TSS) of *ANK1* (variant 1-4). The average difference of methylation in osteosarcoma cell lines versus normal bone samples was 0.36 (DeltaBeta) for CpG79, providing a first evidence for methylation of the miR-486 locus.

We next integrated the expression and methylation level of *miR-486*. An inverse correlation was found between the level of methylation (Beta value) of this CpG site and expression of miR-486-5p (Pearson's correlation (r) of -0.57 (p-value 0.005)). This indicates an association between low expression of miR-486-5p and CpG methylation (Figure 1b).

Demethylation caused increased expression of miR-486-5p

We next examined the effect of changes in methylation on miR-486-5p expression. Osteosarcoma cell lines (n=12) were treated with the demethylation agent 5-Aza. After 72

hours, the relative expression levels of miR-486-5p in untreated and treated cell lines were quantified by qRT-PCR. A significant difference between the cells before and after treatment was observed (p=0.02). miR-486-5p showed at least a 1.5-fold induction in 5/12 tested cell lines (IOR/OS10, MG-63, OHS, OSA and U-2 OS, Figure 2), indicating that the expression of miR-486-5p was affected by changes in DNA methylation.

The genes within the miR-*486/ANK1* locus were not observed to be co-regulated

Several transcript variants of *ANK1* exist, with multiple transcriptional start sites, promoter regions and CGIs. The human *ANK1* variant 9 has the most upstream first exon, and an alternative exon 1 is used in variants 1-4. *sANK1* represents the short variants 5, 7 and 10, whereas alternative exon 1 and exons 41 and 42 are in common with the other transcript variants.

To address the relationship between expression of miR-486-5p and the different *ANK1* transcript variants, qRT-PCR was performed. In osteosarcoma cell lines, *ANK1* variant 1-4 were found to be moderately expressed in 8/12 lines. The *sANK1* variant was only weakly detected in 3/12 cell lines, while variant 9 was undetected (Supplementary Figure 1a).

ANK1 variant 1-4 expression was induced in 8/12 cell lines upon 5-Aza treatment (Supplementary Figure 1b). The *sANK1* variant was only induced in four cell lines and no variant 9 transcripts could be detected upon 5-Aza treatment. No correlation (r=0.2) was seen between expression of miR-486-5p and *ANK1* (variant 1-4) before or after treatment. These observations do not support a co-regulation between miRNA and mRNA genes in the miR 486/ANK1 locus.

Genome-wide methylation profiling revealed hypermethylation of a CGI upstream of *miR-486* in osteosarcoma patient samples

To investigate the methylation level of the whole *miR-486* locus, we performed high resolution Infinium 450k methylation array analysis on a set of 10 osteosarcoma patient samples and four normal bones. For the *mir-486/ANK1* locus, methylation data from 96 CpG sites across all CGIs were determined. The CpG sites located in non-CGI regions were in general hypermethylated in both groups of samples, with a higher level for bone (Figure 3a). Higher methylation levels for osteosarcoma patient samples compared to bone were only observed in the CGI CpG79 (Figure 3a), showing different levels of methylation within the patient cohort (Figure 3b).

The patients samples were classified as unmethylated or methylated based on methylation level of one of the CpG sites that had the most evident methylation in CpG79. A mean Beta value above 0.7 was regarded as methylated and below 0.3 was regarded as unmethylated. In general, miR-486-5p was observed to be low expressed in highly methylated samples and higher expressed in unmethylated samples with a p-value of 0.03 (Figure 3c). This suggests that methylation of an upstream regulatory region affects miR-486-5p expression in osteosarcoma patients.

Qualitative and quantitative methylation analysis confirms hypermethylation of *mir-486* in osteosarcoma

Methylation specific PCR (MSP) analysis was done for CpG79, located upstream of miR-486. The CGI CpG79 was hypermethylated in 20/21 cell lines (Figure 4). Interestingly, this CGI was unmethylated in the IOR/OS14 cell line, previously shown to be globally hypomethylated [10].

Direct bisulfite sequencing was performed on osteosarcoma cell lines. The analysis was done on an extended region of the CGI CpG79, covering a total of 34 CpGs including the region

for the MSP on CpG79 (Figure 4). The resulting data confirmed the methylation status previously determined by MSP.

The methylation of a region of CpG79 of mir-486 was analysed quantitatively by qMSP in a larger cohort of samples, including osteosarcoma cell lines (n=20), xenografts (n=41), patient samples (n=23) and bone (n=5). Methylated PMR was set to >5.2. High qMSP methylation pattern was only observed in cancer samples, comprising both cell lines, xenografts and patient samples (Figure 5). Mann–Whitney U test was used to compare the PMR values of the candidate regions in the different tissues, showing only significant differences between bone and cell lines (p=0.005). For the cell lines, 17/20 (85%) showed increased methylation (>2x) compared to bone average. However, increased methylation was also observed for 14/23 (61%) of the patients samples and 17/41 (41%) of the xenografts. Together, these observations suggest that the CGI CpG79 is highly methylated in osteosarcoma.

Overexpression of miR-486-5p induces morphological changes in osteosarcoma cell lines

To investigate the *in vitro* effect of *miR-486*, we transiently transfected the osteosarcoma cell lines OSA, OHS and U-2 OS with miR-486-5p synthetic miRNA mimics. These cell lines showed the highest level of induction upon 5-Aza treatment. Introduction of miR-486-5p caused a reduced growth rate in OSA and U-2 OS at 48 hours, although the changes were not statistically significant (p=0.2). However, a clear change in cell morphology was observed in all three cell lines where cells became flatter, rounder and smaller (Figure 6). Thus, changes in miR-486-5p levels seem to affect the osteosarcoma cell phenotype.

Discussion

Epigenetic mechanisms such as DNA methylation play crucial roles in controlling miRNA gene expression. Based on our previous observations of a strong, cancer-specific downregulation of miR-486-5p in osteosarcoma cell lines [24], recently confirmed in osteosarcoma patients [26], we set out to investigate the epigenetic regulation of miR-486-5p in osteosarcoma.

In this study, we have shown that the expression of miR-486-5p is differently regulated in osteosarcoma compared to normal bone. A heterogeneity was seen among the patient cohort regarding methylation status. The patients seem to be divided in two groups, one group highly methylated with low expression and a second group with an opposite pattern of low methylation and high expression. One might speculate that the miRNA regulation can be associated with disease aggressiveness, but extensive clinical data was not available for all of the patients in the cohort.

miR-486 is located intragenic within the last intron of *ANK1*, which encodes ankyrin-1. The *mir-486/ANK1* locus is complex, and contains multiple promoter regions and CGIs. Alternative splicing and distinct use of promoters give rise to different isoforms of *ANK1* [37,38]. The methylation of the CGI covering the TSS of *ANK1* variants 1-4 indicates that the miR-486 locus is under control of the *ANK1* gene promoter in this region. This CGI was the only CGI in this locus that was hypermethylated in a high-resolution analysis, and cancer-specific methylation was verified in cancer cell lines, xenografts and clinical samples. In many cases, intergenic miRNAs are co-expressed with their host genes, suggesting that they depend on the same regulatory mechanisms [39,40]. However, no clear evidence of co-expression of *ANK1* and miR-486-5p was seen. This might be explained by the multiple levels of processing that is occurring during mRNA splicing and miRNA biogenesis.

It has been shown that alternative promoters give individualized regulation of transcripts with distinct first exons, providing an expression pattern with a strong tissue

preference [41]. The regulation of the *miR-486/ANK1 locus* may depend on the specific cellular context. The putative host gene *ANK1* is a prototype of the ankyrin membrane proteins, linking integral membrane proteins to the underlying spectrin network in erythroid cells [42], and has also been found in brain and muscles [37,43]. The diversity of the ankyrins suggests that the isoforms might serve different roles in various cell types. An early study showed that *mir-486* can be controlled by an alternative, muscle-specific promoter within intron 40 of the sANK1 variant [44]. The sANK1 isoform could only be detected for a few of the osteosarcoma cell lines in our study, and was only induced in a subset of the cell lines. In myeloid leukemia with an erythroid phenotype, *miR-486* was regulated through *GATA1* binding to the promoter region of *ANK1,* variant 1-4 [45]. An extensive study of miR-486-5p was recently performed in non-small cell lung cancer, showing that miR-486-5p was co-expressed with *ANK1* variant 9 in lung cancer and lung epithelial cells. Aberrant methylation of the CGI covering the TSS of *ANK1* variant 9 (termed ANK1B promoter) repressed both *ANK1* and miR-486-5p [27], and was specific for adenocarcinoma. In our study, this CGI was unmethylated in all the osteosarcoma cell lines and the transcript could not be detected upon 5-Aza treatment.

In our study, induction of miR-486-5p expression in osteosarcoma cells resulted in a change in cell morphology, as well as a pattern of reduced cell proliferation in 2 out of 3 cell lines tested. A morphological change in MG-63 cells following overexpression of miR-486 has been described, possibly related to an EMT-like phenotype [46]. Through *in vitro* experiments it has been shown that miR-486 can reduce proliferation, promote apoptosis and inhibit metastasis through regulation of the PKC-δ pathway in osteosarcoma cells [26]. miR486 also promotes proosteogenic activity through induction of myofibroblastic differentiation through the PTEN–AKT pathway [47]. Following our and others observations of a low expression level of miR-485-5p in cancer, miR-486-5p has been described as a tumour suppressor in breast carcinoma, colorectal cancer, esophageal cancer hepatocellular carcinoma, lung cancer, gastric carcinoma,

myxoid liposarcoma, colorectal cancer, esophageal cancer and lately leukemia [27,48-55]. The functions of miR-486 in cancer cells are controversial, and other reports show that miR-486-5p rather play a causative, oncogenic role, as in other solid tumours like gliomas, prostate and cervical cancer, through negative regulation of multiple tumour suppressor pathways [56-58].

In conclusion, the present study of miR-486-5p shows that the low expression observed for miR-486-5p in osteosarcoma is caused by cancer-specific methylation of an upstream promoter region. This implies a tumor suppressive role of miR-486-5p in osteosarcoma, and the epigenetic regulation should be further correlated with clinical characteristics. The main effect of miR-486-5p over-expression was seen as morphological changes in osteosarcoma cells, and the functional role needs to be further validated in extended model systems.

References

1 Friebele, J. C., Peck, J., Pan, X., Abdel-Rasoul, M. & Mayerson, J. L. Osteosarcoma: A Meta-Analysis and Review of the Literature. *Am J Orthop (Belle Mead NJ)* **44**, 547-553 (2015).

2 Hattinger, C. M., Patrizio, M. P., Magagnoli, F., Luppi, S. & Serra, M. An update on emerging drugs in osteosarcoma: towards tailored therapies? *Expert opinion on emerging drugs* **24**, 153-171, doi:10.1080/14728214.2019.1654455 (2019).

3 Perry, J. A. *et al.* Complementary genomic approaches highlight the PI3K/mTOR pathway as a common vulnerability in osteosarcoma. *Proceedings of the National Academy of Sciences* **111**, E5564 (2014).

4 Kovac, M. *et al.* Exome sequencing of osteosarcoma reveals mutation signatures reminiscent of BRCA deficiency. *Nat Commun* **6**, 8940, doi:10.1038/ncomms9940 (2015).

5 Lorenz, S. *et al.* Unscrambling the genomic chaos of osteosarcoma reveals extensive transcript fusion, recurrent rearrangements and frequent novel TP53 aberrations. *Oncotarget*, doi:10.18632/oncotarget.6567 (2015).

6 Behjati, S. *et al.* Recurrent mutation of IGF signalling genes and distinct patterns of genomic rearrangement in osteosarcoma. *Nature Communications* **8**, 15936, doi:10.1038/ncomms15936 (2017).

7 Hattinger, C. M., Patrizio, M. P., Luppi, S. & Serra, M. Pharmacogenomics and Pharmacogenetics in Osteosarcoma: Translational Studies and Clinical Impact. *Int J Mol Sci* **21**, doi:10.3390/ijms21134659 (2020).

8 Hattinger, C. M. *et al.* Genetic testing for high-grade osteosarcoma: a guide for future tailored treatments? *Expert Rev Mol Diagn* **18**, 947-961, doi:10.1080/14737159.2018.1535903 (2018).

9 Sadikovic, B. *et al.* Identification of Interactive Networks of Gene Expression Associated with Osteosarcoma Oncogenesis by Integrated Molecular Profiling. *Human molecular genetics* **18**, 1962-1975 (2009).

10 Kresse, S. H. *et al.* Integrative Analysis Reveals Relationships of Genetic and Epigenetic Alterations in Osteosarcoma. *PLoS ONE* **7**, e48262 (2012).

11 Mills, L. J. *et al.* Comparative analysis of genome-wide DNA methylation identifies patterns that associate with conserved transcriptional programs in osteosarcoma. *Bone*, 115716, doi:10.1016/j.bone.2020.115716 (2020).

12 Shu, J. *et al.* Imprinting defects at human 14q32 locus alters gene expression and is associated with the pathobiology of osteosarcoma. *Oncotarget* **7**, 21298-21314, doi:10.18632/oncotarget.6965 (2016).

13 Asano, N. *et al.* Epigenetic reprogramming underlies efficacy of DNA demethylation therapy in osteosarcomas. *Sci Rep* **9**, 20360, doi:10.1038/s41598-019-56883-0 (2019).

14 Li, B. & Ye, Z. Epigenetic alterations in osteosarcoma: promising targets. *Mol Biol Rep* **41**, 3303-3315, doi:10.1007/s11033-014-3193-7 (2014).

15 Kulis, M. & Esteller, M. DNA methylation and cancer. *Adv Genet* **70**, 27-56, doi:10.1016/B978-0-12-380866-0.60002-2 (2010).

16 Berdasco, M. & Esteller, M. Clinical epigenetics: seizing opportunities for translation. *Nature Reviews Genetics* **20**, 109-127, doi:10.1038/s41576-018-0074-2 (2019).

17 Michalak, E. M., Burr, M. L., Bannister, A. J. & Dawson, M. A. The roles of DNA, RNA and histone methylation in ageing and cancer. *Nature Reviews Molecular Cell Biology* **20**, 573-589, doi:10.1038/s41580-019-0143-1 (2019).

18 Saxonov, S., Berg, P. & Brutlag, D. L. A genome-wide analysis of CpG dinucleotides in the human genome distinguishes two distinct classes of promoters. *Proceedings of the National Academy of Sciences* **103**, 1412, doi:10.1073/pnas.0510310103 (2006).
19 Suzuki, M. M. & Bird, A. DNA methylation landscapes: provocative insights from epigenomics. *Nature reviews* **9**, 465-476 (2008).
20 Yao, Q., Chen, Y. & Zhou, X. The roles of microRNAs in epigenetic regulation. *Curr Opin Chem Biol* **51**, 11-17, doi:10.1016/j.cbpa.2019.01.024 (2019).
21 Weber, B., Stresemann, C., Brueckner, B. & Lyko, F. Methylation of human microRNA genes in normal and neoplastic cells. *Cell cycle (Georgetown, Tex* **6**, 1001-1005 (2007).
22 Maire, G. *et al.* Analysis of miRNA-gene expression-genomic profiles reveals complex mechanisms of microRNA deregulation in osteosarcoma. *Cancer Genetics* **204**, 138-146, doi:10.1016/j.cancergen.2010.12.012 (2011).
23 Jones, K. B. *et al.* MicroRNA signatures associate with pathogenesis and progression of osteosarcoma. *Cancer research* **72**, 1865-1877, doi:10.1158/0008-5472.CAN-11-2663 (2012).
24 Namløs, H. M. *et al.* Modulation of the Osteosarcoma Expression Phenotype by MicroRNAs. *PLoS ONE* **7**, e48086 (2012).
25 Lietz, C. E. *et al.* MicroRNA-mRNA networks define translatable molecular outcome phenotypes in osteosarcoma. *Sci Rep* **10**, 4409, doi:10.1038/s41598-020-61236-3 (2020).
26 He, M. *et al.* miR-486 suppresses the development of osteosarcoma by regulating PKC-δ pathway. *International Journal of Oncology* **50**, 1590-1600, doi:10.3892/ijo.2017.3928 (2017).
27 Tessema, M. *et al.* ANK1 Methylation regulates expression of MicroRNA-486-5p and discriminates lung tumors by histology and smoking status. *Cancer letters* **410**, 191-200, doi:doi.org/10.1016/j.canlet.2017.09.038 (2017).
28 Ottaviano, L. *et al.* Molecular characterization of commonly used cell lines for bone tumor research: a trans-European EuroBoNet effort. *Genes, chromosomes & cancer* **49**, 40-51 (2010).
29 Lauvrak, S. U. *et al.* Functional characterisation of osteosarcoma cell lines and identification of mRNAs and miRNAs associated with aggressive cancer phenotypes. *Br J Cancer* **109**, 2228-2236, doi:10.1038/bjc.2013.549 (2013).
30 Mayordomo, E. *et al.* A tissue microarray study of osteosarcoma: histopathologic and immunohistochemical validation of xenotransplanted tumors as preclinical models. *Appl Immunohistochem Mol Morphol* **18**, 453-461 (2010).
31 Kresse, S. H., Meza-Zepeda, L. A., Machado, I., Llombart-Bosch, A. & Myklebost, O. Preclinical xenograft models of human sarcoma show nonrandom loss of aberrations. *Cancer* **118**, 558-570, doi:10.1002/cncr.26276 (2012).
32 Raymond, A. K., Ayala, A. G. & Knuutila, S. in *World Health Organization Classification of Tumours. Pathology and Genetics of Tumours of Soft Tissue and Bone* (eds C.D.M. Fletcher, K.K. Unni, & F. Mertens) (IARC Press, 2002).
33 Lind, G. E. *et al.* Identification of an epigenetic biomarker panel with high sensitivity and specificity for colorectal cancer and adenomas. *Molecular cancer* **10**, 85 (2011).
34 Lind, G. E. *et al.* Hypermethylated MAL gene - a silent marker of early colon tumorigenesis. *Journal of translational medicine* **6**, 13 (2008).
35 Melki, J. R., Vincent, P. C. & Clark, S. J. Concurrent DNA hypermethylation of multiple genes in acute myeloid leukemia. *Cancer research* **59**, 3730-3740 (1999).

36 Widschwendter, M. *et al.* Association of breast cancer DNA methylation profiles with hormone receptor status and response to tamoxifen. *Cancer research* **64**, 3807-3813 (2004).
37 Gallagher, P. G. & Forget, B. G. An alternate promoter directs expression of a truncated, muscle-specific isoform of the human ankyrin 1 gene. *The Journal of biological chemistry* **273**, 1339-1348 (1998).
38 Gallagher, P. G., Romana, M., Tse, W. T., Lux, S. E. & Forget, B. G. The human ankyrin-1 gene is selectively transcribed in erythroid cell lines despite the presence of a housekeeping-like promoter. *Blood* **96**, 1136-1143 (2000).
39 Baskerville, S. & Bartel, D. P. Microarray profiling of microRNAs reveals frequent coexpression with neighboring miRNAs and host genes. *RNA (New York, N.Y* **11**, 241-247 (2005).
40 Hinske, L. C. G., Galante, P. A. F., Kuo, W. P. & Ohno-Machado, L. A potential role for intragenic miRNAs on their hosts' interactome. *BMC genomics* **11**, 533-533, doi:10.1186/1471-2164-11-533 (2010).
41 Jacox, E., Gotea, V., Ovcharenko, I. & Elnitski, L. Tissue-Specific and Ubiquitous Expression Patterns from Alternative Promoters of Human Genes. *PLoS ONE* **5**, e12274, doi:10.1371/journal.pone.0012274 (2010).
42 Bennett, V. & Lorenzo, D. N. in *Current Topics in Membranes* Vol. 72 (ed Vann Bennett) 1-37 (Academic Press, 2013).
43 Lunnon, K. *et al.* Cross-tissue methylomic profiling strongly implicates a role for cortex-specific deregulation of ANK1 in Alzheimer's disease neuropathology. *Nature neuroscience* **17**, 1164-1170, doi:10.1038/nn.3782 (2014).
44 Small, E. M. *et al.* Regulation of PI3-kinase/Akt signaling by muscle-enriched microRNA-486. *Proceedings of the National Academy of Sciences of the United States of America* **107**, 4218-4223 (2010).
45 Shaham, L. *et al.* MicroRNA-486-5p is an erythroid oncomiR of the myeloid leukemias of Down syndrome. *Blood* **125**, 1292-1301, doi:10.1182/blood-2014-06-581892 (2015).
46 Liu, H. *et al.* miR-486 inhibited osteosarcoma cells invasion and epithelial-mesenchymal transition by targeting PIM1. *Cancer Biomark*, doi:10.3233/CBM-181527 (2018).
47 Song, R. *et al.* Altered MicroRNA Expression Is Responsible for the Pro-Osteogenic Phenotype of Interstitial Cells in Calcified Human Aortic Valves. *Journal of the American Heart Association: Cardiovascular and Cerebrovascular Disease* **6**, e005364, doi:10.1161/JAHA.116.005364 (2017).
48 Liu, H., Ni, Z., Shi, L., Ma, L. & Zhao, J. MiR-486-5p inhibits the proliferation of leukemia cells and induces apoptosis through targeting FOXO1. *Molecular and Cellular Probes* **44**, 37-43, doi:https://doi.org/10.1016/j.mcp.2019.02.001 (2019).
49 Oh, H. K. *et al.* Genomic Loss of miR-486 Regulates Tumor Progression and the OLFM4 Antiapoptotic Factor in Gastric Cancer. *Clin Cancer Res* **17**, 2657-2667 (2011).
50 Borjigin, N. *et al.* TLS-CHOP represses miR-486 expression, inducing upregulation of a metastasis regulator PAI-1 in human myxoid liposarcoma. *Biochemical and Biophysical Research Communications* (2012).
51 Peng, Y. *et al.* Insulin growth factor signaling is regulated by microRNA-486, an underexpressed microRNA in lung cancer. *Proceedings of the National Academy of Sciences* **110**, 15043-15048, doi:10.1073/pnas.1307107110 (2013).
52 Zhang, G., Liu, Z., Cui, G., Wang, X. & Yang, Z. MicroRNA-486-5p targeting PIM-1 suppresses cell proliferation in breast cancer cells. *Tumor Biol.* **35**, 11137-11145, doi:10.1007/s13277-014-2412-0 (2014).

53 Liu, X. *et al.* DNA-methylation-mediated silencing of miR-486-5p promotes colorectal cancer proliferation and migration through activation of PLAGL2/IGF2/β-catenin signal pathways. *Cell death & disease* **9**, 1037-1037, doi:10.1038/s41419-018-1105-9 (2018).
54 Lang, B. & Zhao, S. miR-486 functions as a tumor suppressor in esophageal cancer by targeting CDK4/BCAS2. *Oncology reports* **39**, 71-80, doi:10.3892/or.2017.6064 (2018).
55 Huang, X.-P. *et al.* MicroRNA-486-5p, which is downregulated in hepatocellular carcinoma, suppresses tumor growth by targeting PIK3R1. *FEBS Journal* **282**, 579-594, doi:10.1111/febs.13167 (2015).
56 Tetzlaff, M. T., Curry, J. L., Yin, V. & et al. DIstinct pathways in the pathogenesis of sebaceous carcinomas implicated by differentially expressed micrornas. *JAMA Ophthalmology*, doi:10.1001/jamaophthalmol.2015.2310 (2015).
57 Yang, Y. *et al.* The miR-486-5p plays a causative role in prostate cancer through negative regulation of multiple tumor suppressor pathways. *Oncotarget* **8**, 72835-72846, doi:10.18632/oncotarget.20427 (2017).
58 Li, C. *et al.* Serum miR-486-5p as a diagnostic marker in cervical cancer: with investigation of potential mechanisms. *BMC cancer* **18**, 61, doi:10.1186/s12885-017-3753-z (2018).

Data availability

For the microarray experiments, MIAME compliant data can be downloaded from the GEO data repository (www.ncbi.nlm.nih.gov/geo/). The Agilent Human miRNA Microarray datasets are deposited under the accession number GSE28425, the Illumina HumanMethylation27 datasets under the accession number GSE36002 in SuperSeries number GSE36004 and the Infinium HumanMethylation450 DNA methylation datasets under the accession number GSE161407.

Supplementary material

Supplementary Tables and Figures are available in the online version of the article.

Acknowledgements

We appreciate the help of Thea C. Smedsrud (Oslo University Hospital Genomics Core Facility) for performing the Infinium HumanMethylation450 BeadChip experiments.

The study was funded by EuroBoNet, a European Commission granted Network of Excellence for studying the pathology and genetics of bone tumours (LSHC-CT-2006-018814), the Norwegian Cancer Society grant number PR-2007-0163 and the Ragnvarda F. Sørvik and Håkon Starheims legacy. No potential conflicts of interest were disclosed.

Authors contributions

HMN, M. Skårn, IG, DA, KA and SHK performed the experiments. HMN, M. Skårn, DA, GEL and LAMZ carried out experimental analyses and data interpretation. HMN, M. Skårn, GEL and LAMZ contributed to the study design. HMN and M. Skårn drafted the manuscript. OM, M. Serra, KS and ALB provided osteosarcoma samples. LAMZ and OM conceived of the study. All authors have approved the final manuscript.

Competing interests

The authors declare no competing interests.

Figures

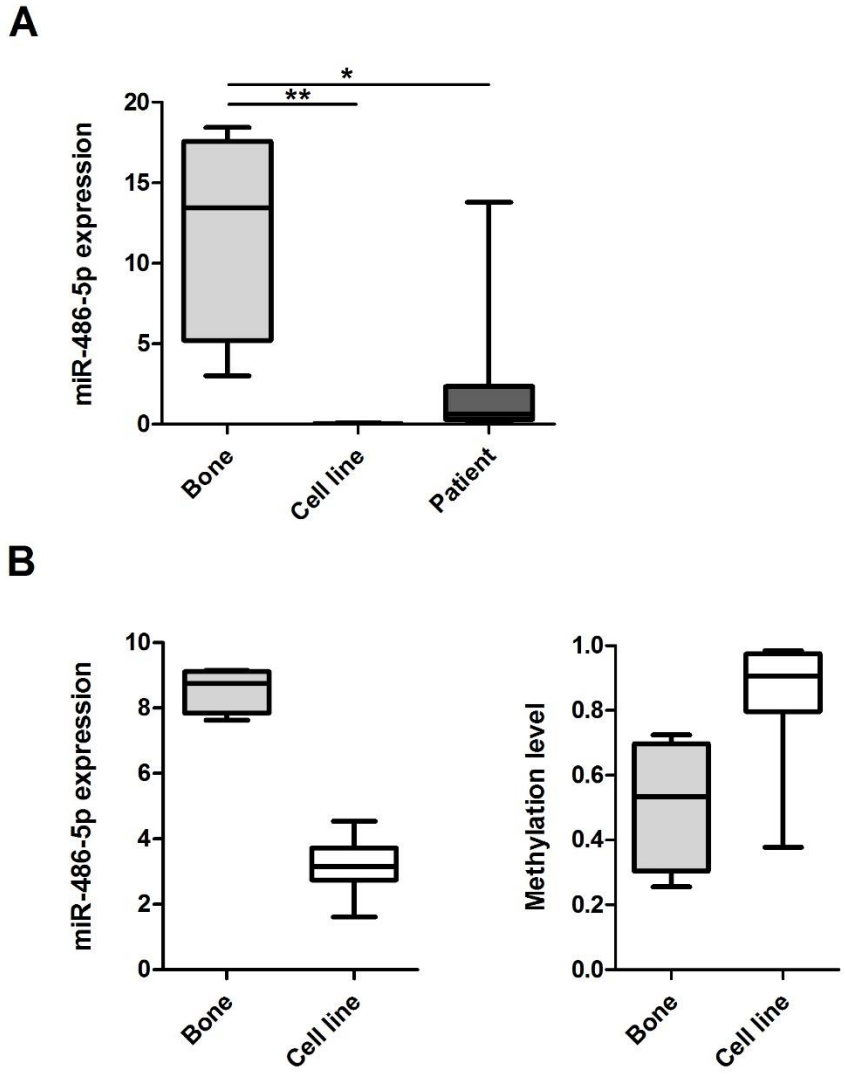

Figure 1. miR-486-5p expression and methylation in osteosarcoma cell lines and patient samples. A. miR-486-5p expression level in normal bone (n=4), cell lines (n=17) and patient samples (n=10) using qRT-PCR. The expression level was quantified for the groups of samples. **B**. DNA methylation and miRNA expression levels in normal bone samples (n=4) and osteosarcoma cell lines (n=19) using arrays. A high inverse correlation between the level of expression of miRNAs (log2) and DNA methylation (Beta, probe cg00176210) across the sample panel was identified using Agilent miRNA array v2 and Illumina Infinium Methylation27 BeadChip technology. Values are given as mean (SD) with whiskers from min to max. P-values * <0.01, **<0.0001.

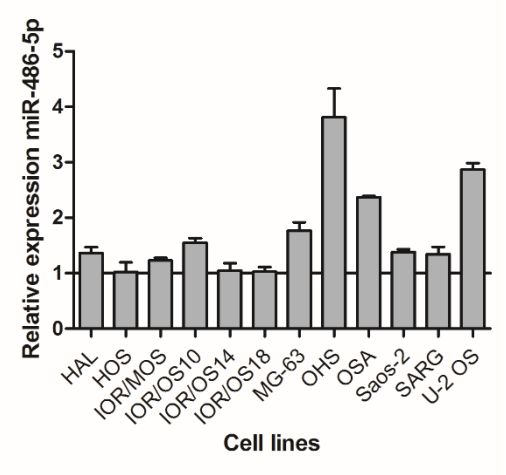

Figure 2. Treatment with 5-Aza-2′-deoxycytidine in cell lines. Quantification of mature miR-486-5p using qRT-PCR in cell lines after treatment with 5-Aza. Expression is shown relative to untreated cells (set to 1, horizontal line). Values are given as mean (SD).

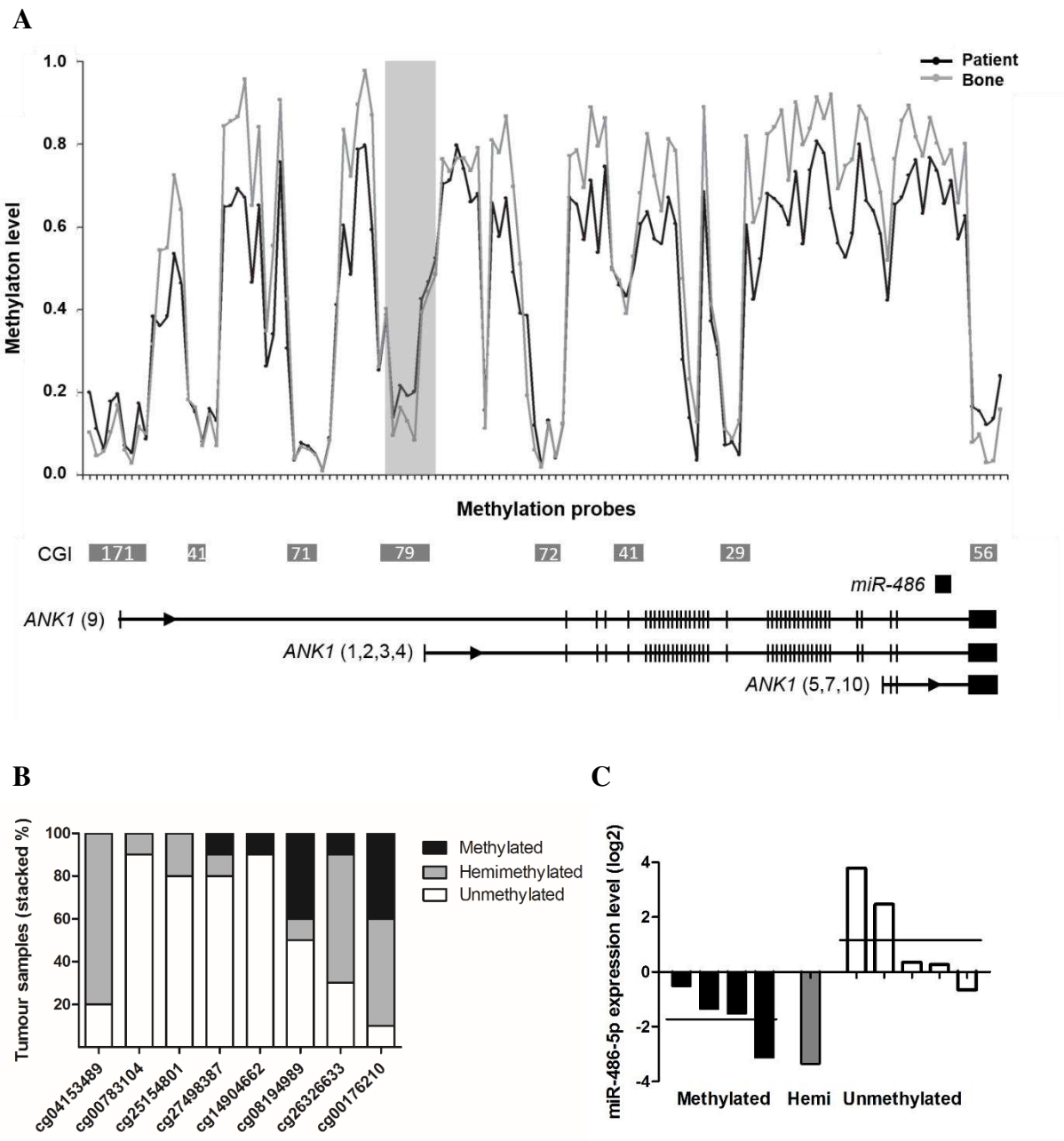

Figure 3. Genome-wide methylation profile of the *miR-486/ANK1* locus and miR-486-5p expression levels in osteosarcoma patient samples

A. Representation of average methylation profile across the *mir-486/ANK1* locus in osteosarcoma patient samples (n=10) and bone (n=4). Methylation level (Beta) is shown for the individual CpG sites (ticks on horizontal axis) from the HumanMethylation450 BeadChips. The probes are ordered along the locus and intervals are not in scale. CGIs are shown as grey boxes with number refering to CpG count (from UCSC Genome Browser). Horizontal lines below plot show representative transcript variants of the respective mRNA genes (RefSeq) with exons as vertical bars, not in scale. Shaded vertical box: CGI shown in detail in B. Black, osteosarcomas; Grey, bone.

B. Probe level methylation for CGI CpG79 in osteosarcoma patient samples. Methylation levels as determined by Infinium 450k arrays are given in Beta values for the individual CpG sites

(cg). The selected CpGs within CGI 79 are highlighted with a shaded vertical box in A. Methylated: Beta 0.7-1.0; hemimethylated: Beta 0.3-0.7; unmethylated: Beta <0.3.
C. Expression level of miR-486-5p in osteosarcoma patient samples based on qRT-PCR. The samples are grouped based on methylation status for probe cg08194989 on Infinium 450k arrays. Horizontal line: mean value.

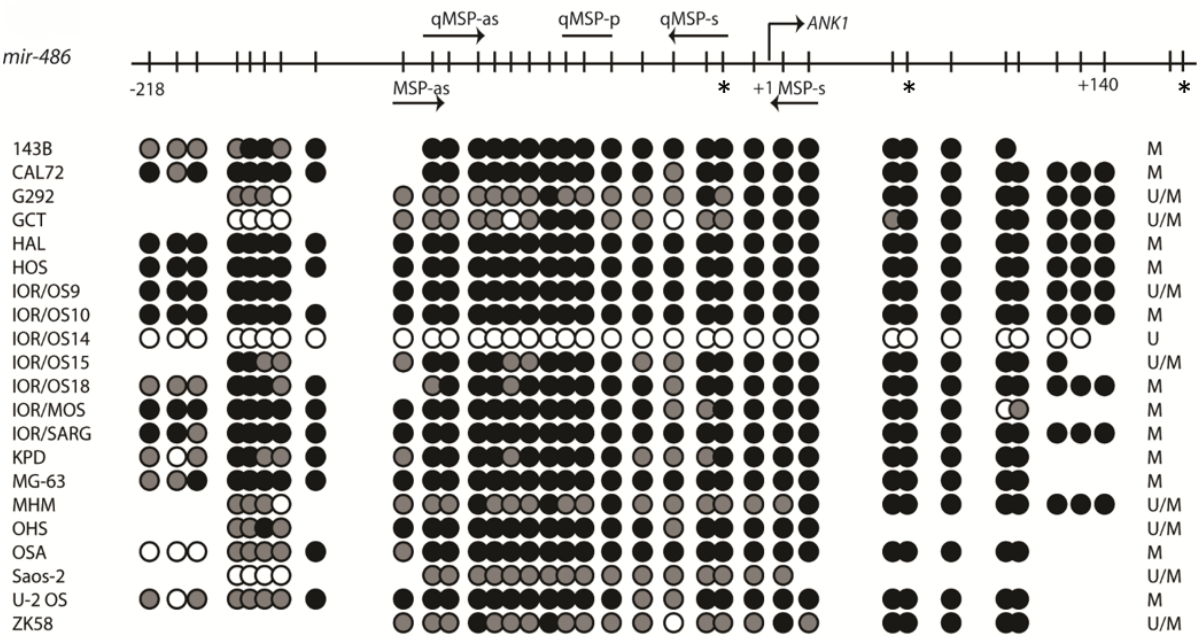

Figure 4. Cell line methylation status of CGI CpG79 located upstream of miR-486 as assessed by methylation specific PCR and direct bisulfite sequencing. The upper part is a schematic presentation of the CpG sites (vertical bars) amplified by the bisulfite sequencing primers. The transcription start site (+1) refers to the start of *ANK1* (transcript variants 1-4). Arrows indicate location of MSP and qMSP primers, * represents the CpGs covered by the Infinium 450k methylation array (cg08194989, cg26326633, cg00176210, respectively). For the lower part of the panel, black circles represent methylated CpGs (>80% cytosine); grey circles represent partially methylated sites (20-80% cytosine) and white circles represent unmethylated sites (<20% cytosine). The column to the right lists the methylation status of the respective cell lines as assessed by MSP analyses.

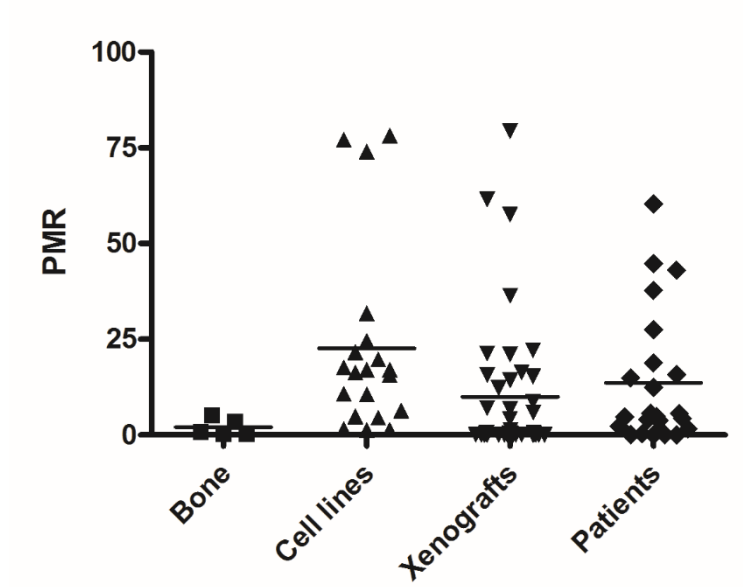

Figure 5. Methylation distributions in the analyzed sample cohorts assessed by quantitative methylation-specific PCR. The methylation was measured for the groups of normal bones and osteosarcoma cell lines, xenografts and patient samples. PMR, percent of methylated reference. Horizontal black line: mean values.

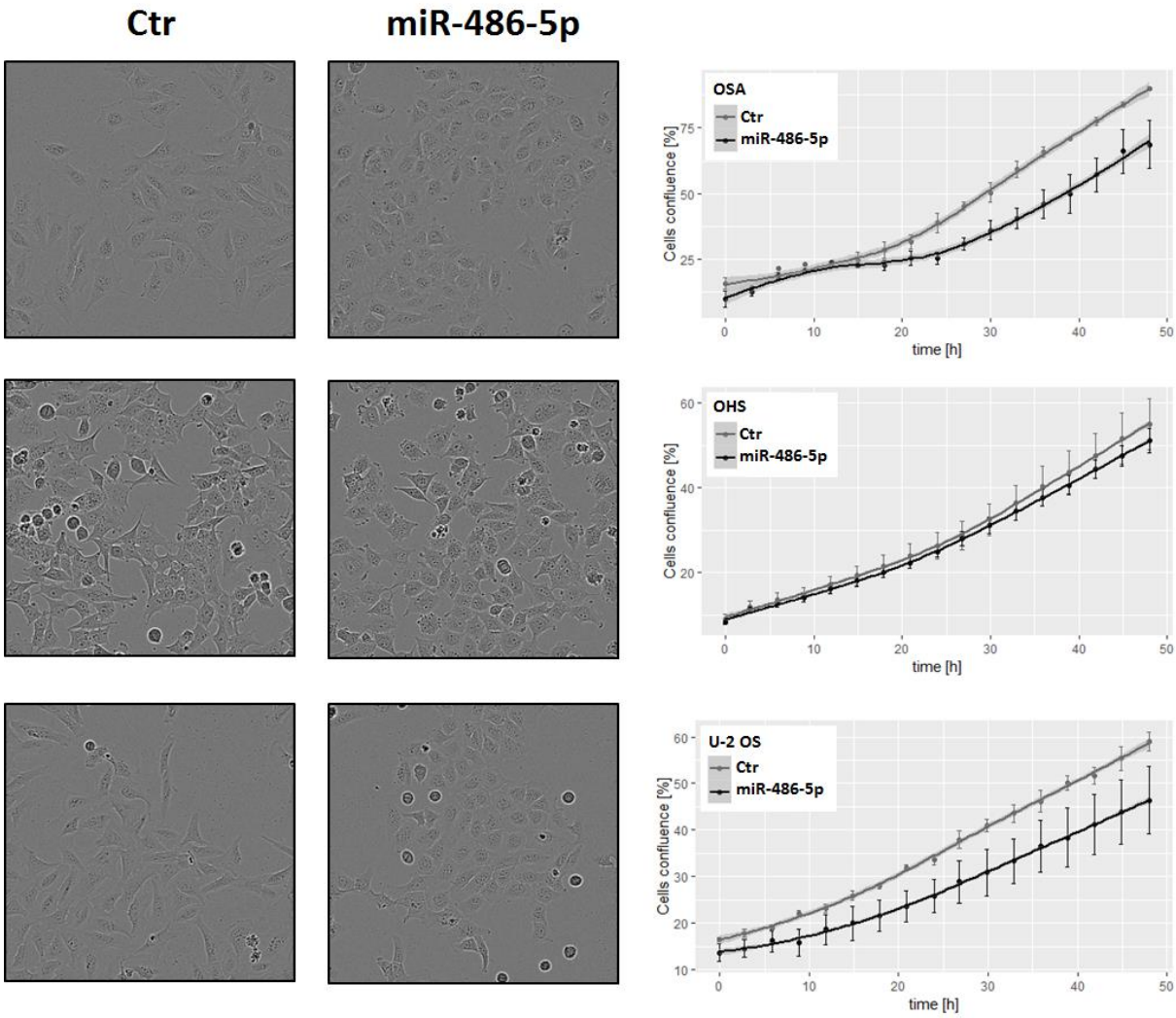

Figure 6. Introduction of miR-486-5p in osteosarcoma cell lines. Osteosarcoma cells (OSA, OHS and U-2 OS) were transiently transfected with synthetic miR-486-5p mimics or a negative control. Cellular proliferation rates were determined by live cell imaging for 48 hours using the IncuCyte, measuring cell confluence over time. One representative experiment of three is shown (n=3). Error bars represent the standard error of means of values for replicate wells (n≥=5).

Figures

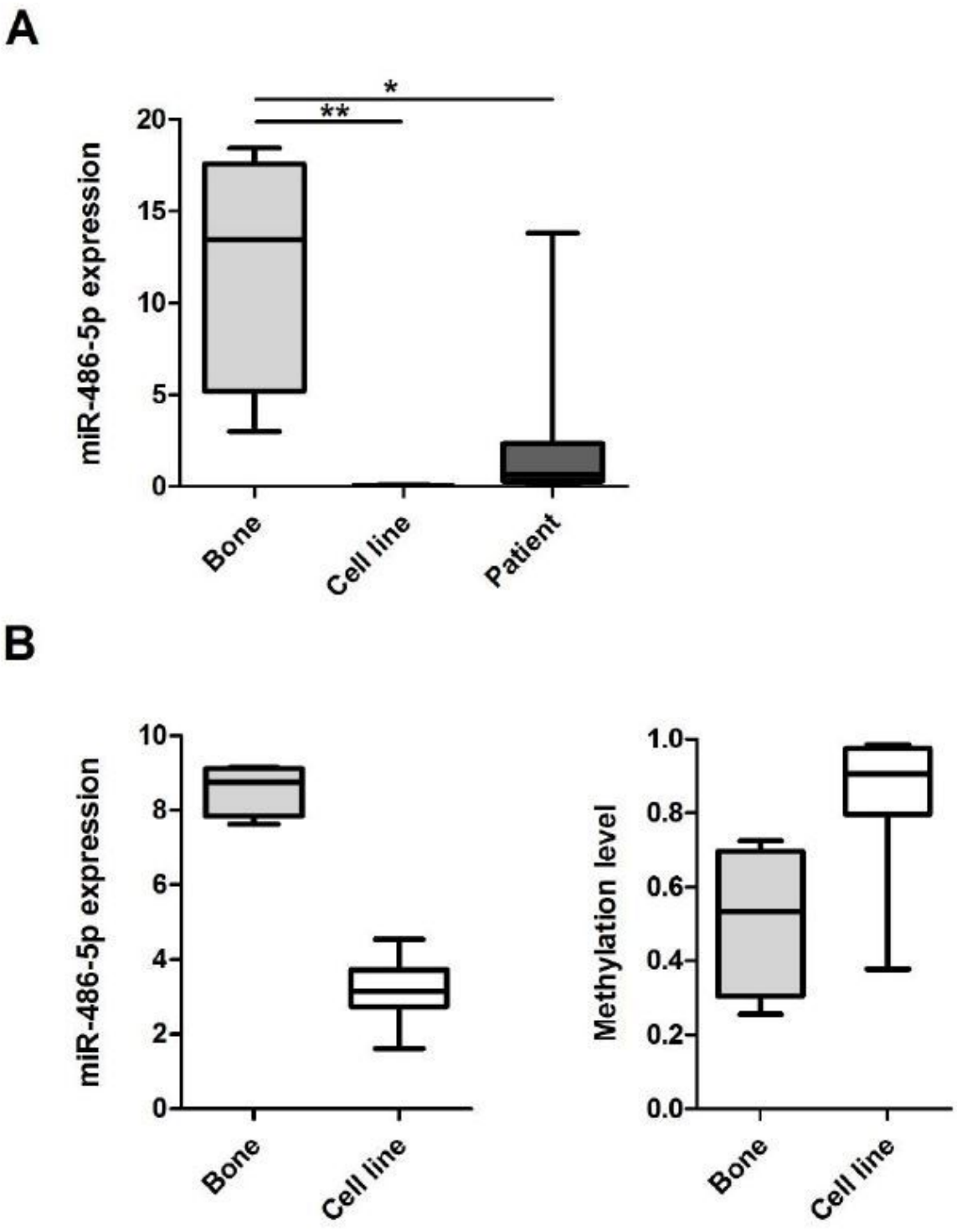

Figure 1

miR-486-5p expression and methylation in osteosarcoma cell lines and patient samples. A. miR-486-5p expression level in normal bone (n=4), cell lines (n=17) and patient samples (n=10) using qRT-PCR. The expression level was quantified for the groups of samples. B. DNA methylation and miRNA expression

levels in normal bone samples (n=4) and osteosarcoma cell lines (n=19) using arrays. A high inverse correlation between the level of expression of miRNAs (log2) and DNA methylation (Beta, probe cg00176210) across the sample panel was identified using Agilent miRNA array v2 and Illumina Infinium Methylation27 BeadChip technology. Values are given as mean (SD) with whiskers from min to max. P-values * <0.01, **<0.0001.

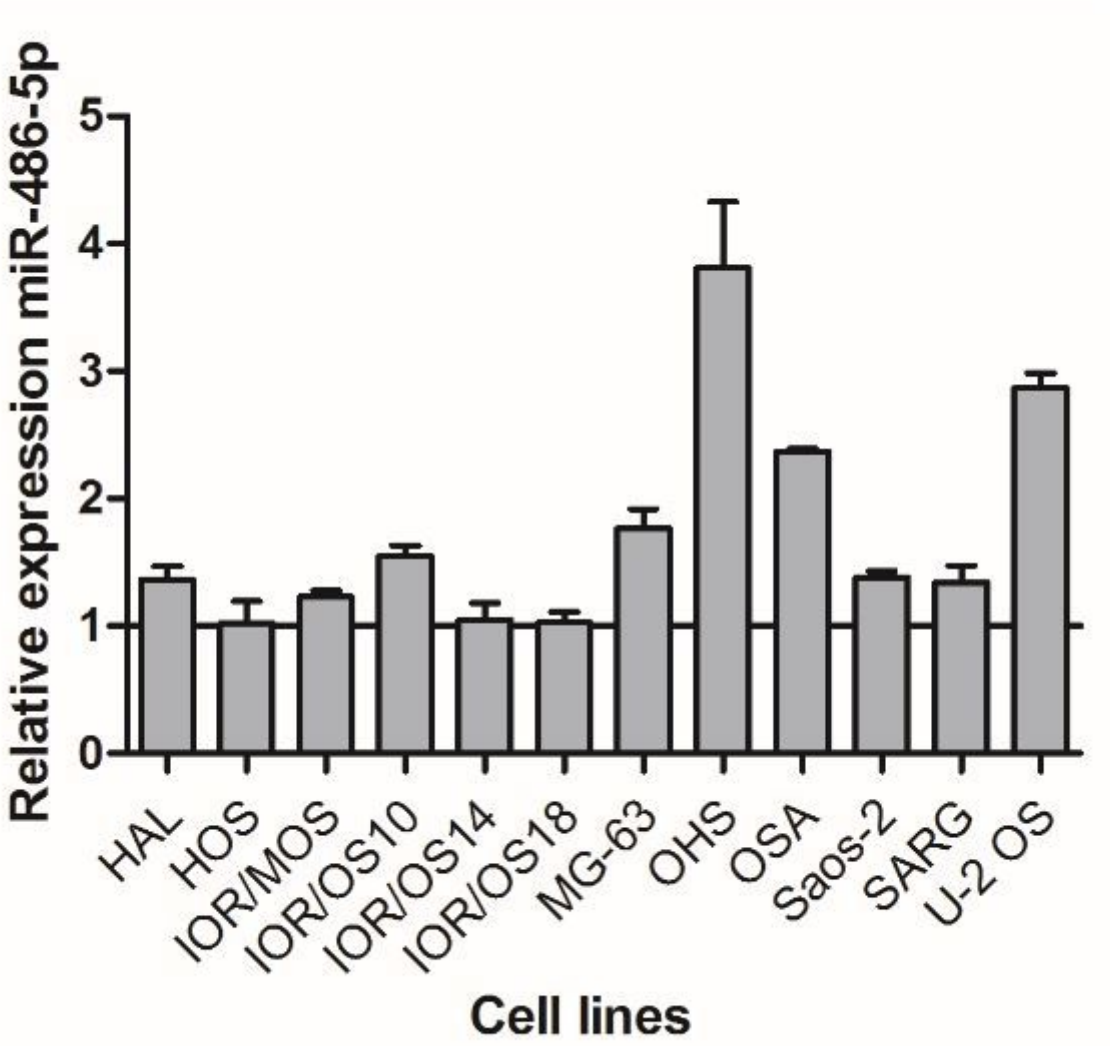

Figure 2

Treatment with 5-Aza-2'-deoxycytidine in cell lines. Quantification of mature miR-486-5p using qRT-PCR in cell lines after treatment with 5-Aza. Expression is shown relative to untreated cells (set to 1, horizontal line). Values are given as mean (SD).

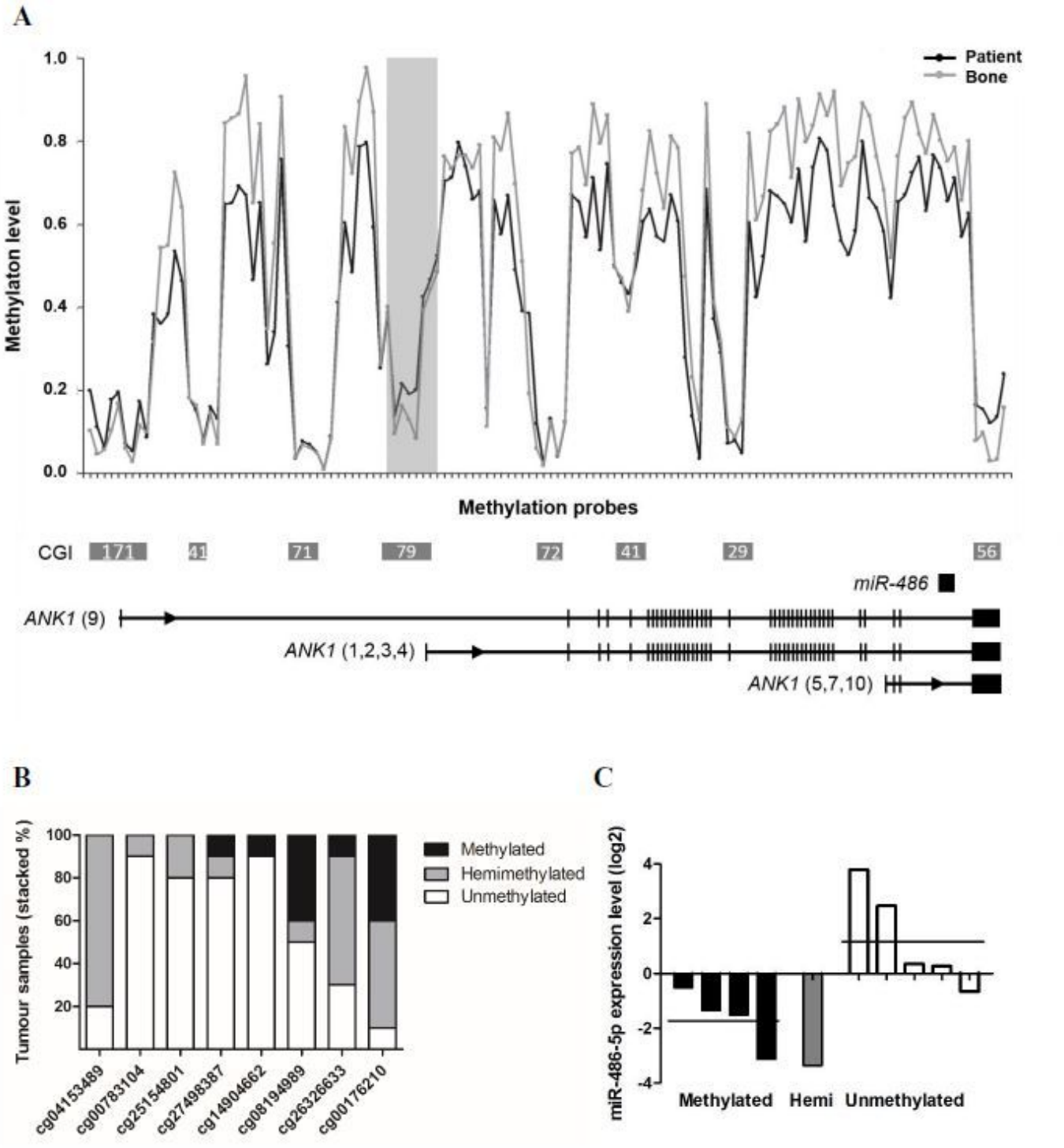

Figure 3

Genome-wide methylation profile of the miR-486/ANK1 locus and miR-486-5p expression levels in osteosarcoma patient samples A. Representation of average methylation profile across the mir-486/ANK1 locus in osteosarcoma patient samples (n=10) and bone (n=4). Methylation level (Beta) is shown for the individual CpG sites (ticks on horizontal axis) from the HumanMethylation450 BeadChips. The probes are ordered along the locus and intervals are not in scale. CGIs are shown as grey boxes with

number refering to CpG count (from UCSC Genome Browser). Horizontal lines below plot show representative transcript variants of the respective mRNA genes (RefSeq) with exons as vertical bars, not in scale. Shaded vertical box: CGI shown in detail in B. Black, osteosarcomas; Grey, bone. B. Probe level methylation for CGI CpG79 in osteosarcoma patient samples. Methylation levels as determined by Infinium 450k arrays are given in Beta values for the individual CpG sites (cg). The selected CpGs within CGI 79 are highlighted with a shaded vertical box in A. Methylated: Beta 0.7-1.0; hemimethylated: Beta 0.3-0.7; unmethylated: Beta <0.3. C. Expression level of miR-486-5p in osteosarcoma patient samples based on qRT-PCR. The samples are grouped based on methylation status for probe cg08194989 on Infinium 450k arrays. Horizontal line: mean value.

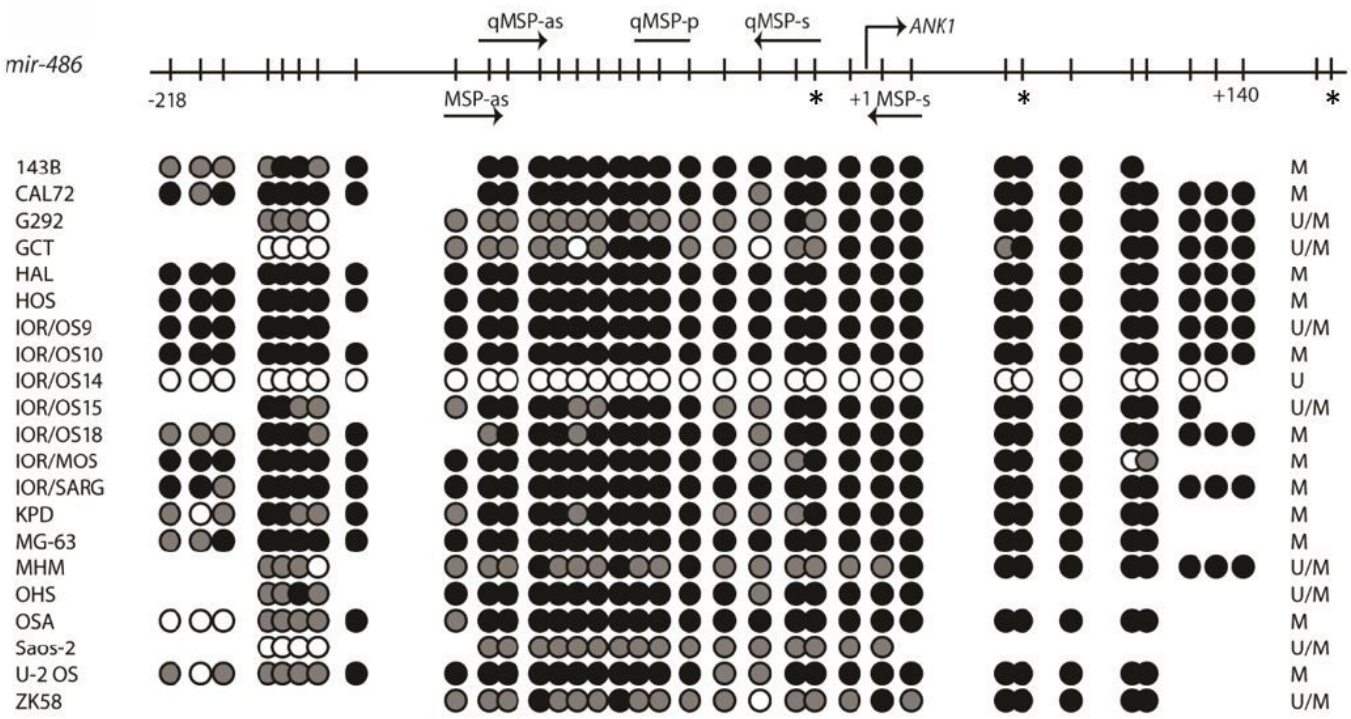

Figure 4

Cell line methylation status of CGI CpG79 located upstream of miR-486 as assessed by methylation specific PCR and direct bisulfite sequencing. The upper part is a schematic presentation of the CpG sites (vertical bars) amplified by the bisulfite sequencing primers. The transcription start site (+1) refers to the start of ANK1 (transcript variants 1-4). Arrows indicate location of MSP and qMSP primers, * represents the CpGs covered by the Infinium 450k methylation array (cg08194989, cg26326633, cg00176210, respectively). For the lower part of the panel, black circles represent methylated CpGs (>80% cytosine); grey circles represent partially methylated sites (20-80% cytosine) and white circles represent unmethylated sites (<20% cytosine). The column to the right lists the methylation status of the respective cell lines as assessed by MSP analyses.

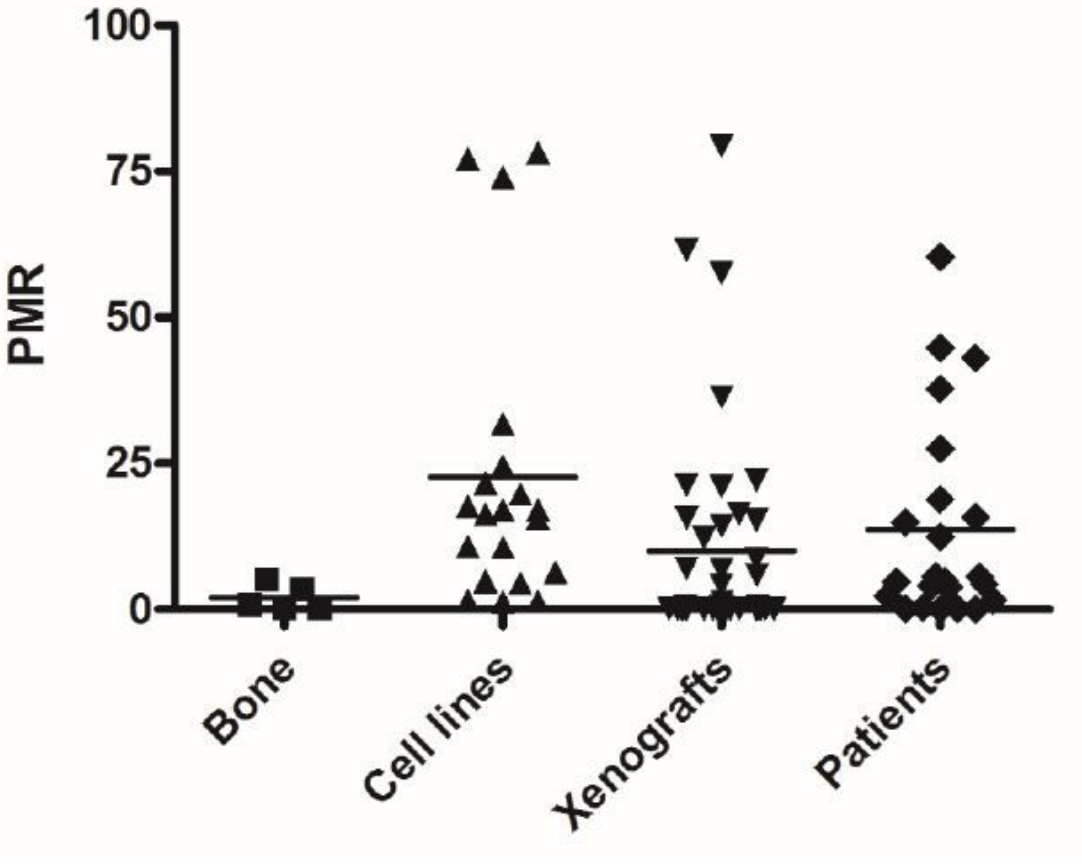

Figure 5

Methylation distributions in the analyzed sample cohorts assessed by quantitative methylation-specific PCR. The methylation was measured for the groups of normal bones and osteosarcoma cell lines, xenografts and patient samples. PMR, percent of methylated reference. Horizontal black line: mean values.

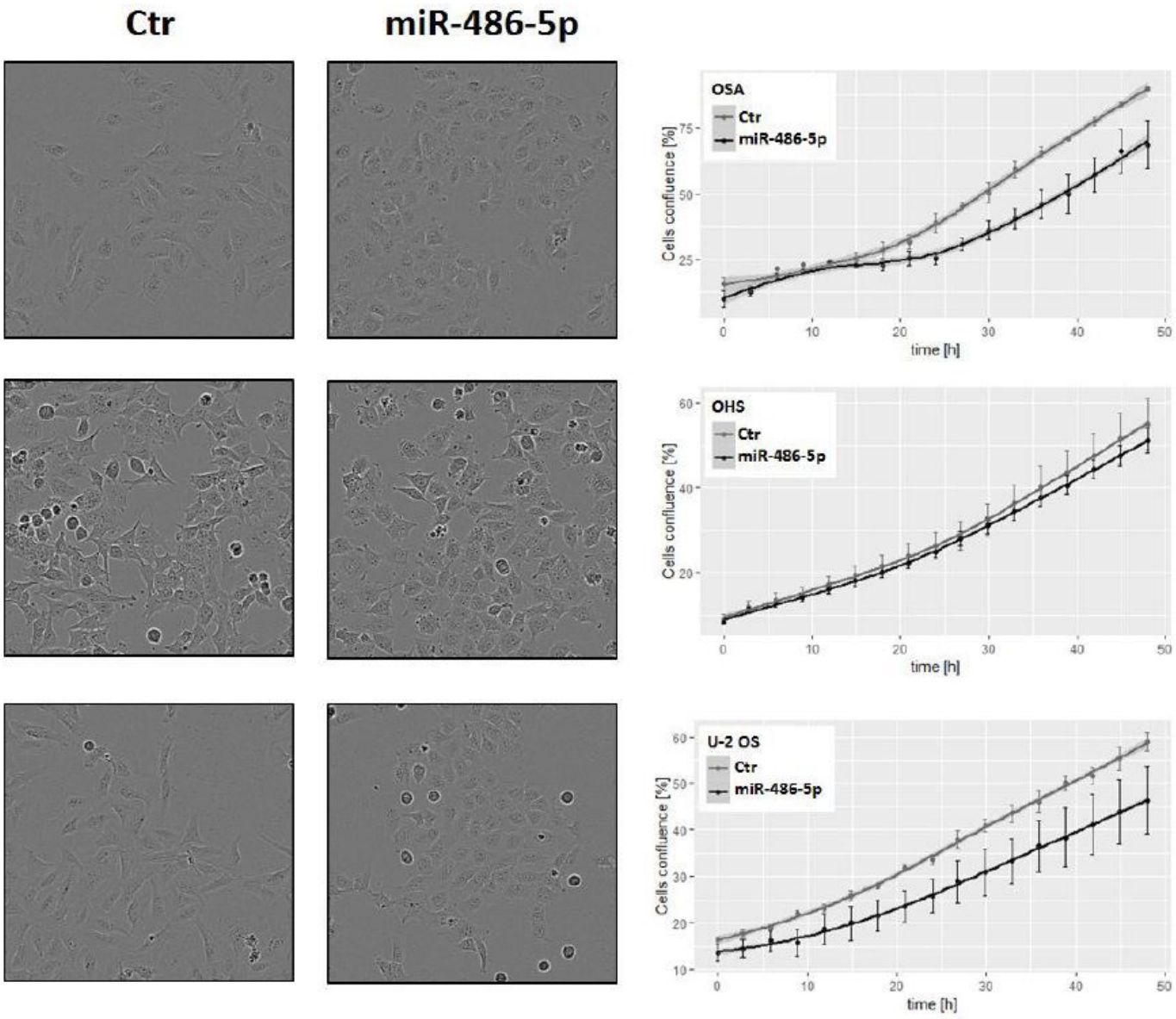

Figure 6

Introduction of miR-486-5p in osteosarcoma cell lines. Osteosarcoma cells (OSA, OHS and U-2 OS) were transiently transfected with synthetic miR-486-5p mimics or a negative control. Cellular proliferation rates were determined by live cell imaging for 48 hours using the IncuCyte, measuring cell confluence over time. One representative experiment of three is shown (n=3). Error bars represent the standard error of means of values for replicate wells (n≥=5).

Supplementary Files

This is a list of supplementary files associated with this preprint. Click to download.

- NamlosSupplementary.pdf